International Journal of Engineering Trends and Technology
ISSN: 2231 – 5381 /doi:10.14445/22315381/IJETT-V69I12P222
Volume 69 Issue 12, 188-196, December, 2021

Original Article

Optimal Design of Controller for Automatic Generation Control in Multi Area Restructured Power System with Battery Energy Storage and Wind Energy Systems

Mr. Ashfaq Ur Rehman Mohamed Riazuddin[1], Dr.Mahabuba Abdulrahim[2], Dr.Jennathu Beevi Sahul Hameed[3], Dr. Jayashree Ramasubramaniam[4]

[1]*Graduate Student of Electrical Engineering-Smart Grid, Politecnico Di Milano, Milan, Italy*
[2]*Electrical Engineering Faculty Member, Dubai Men's College Higher Colleges of Technology, Dubai, U.A.E*
[3]*Assistant Professor (SG), Department of Electrical and Electronics Engineering, B.S. Abdur Rahman Crescent Institute of Science and Technology, Chennai, India*
[4]*Professor, Department of Electrical and Electronics Engineering, B.S. Abdur Rahman Crescent Institute of Science and Technology, Chennai, India*

ashfaqurmr001@gmail.com

Abstract *- In this journal, an attempt to introduce distributed generation units has been made to analyze its impact on the frequency control in restructured power systems replicating the real energy market scenario. The introduction of wind generation system and BESS (Battery Energy Storage System) into the restructured power system along with non-reheat thermal power generating plants is the main objective in order to diversify the generating capacity. The proposed restructured Power system is regulated with proportional Integral Derivatives (PID) and Fractional Order Proportional Integral Derivative (FOPID) Controllers. To reduce The Integral Square Error (ISE), the controller gains are derived using the Genetic Algorithm (GA) and Moth Flame Algorithm (MFO). For the unilateral and bilateral market structures of the system,2 the frequency deviations in both areas, tie-line power variations are analyzed, and performance attributes are compared. Using PID and FOPID controllers, the efficacy of wind and BESS is accessed for the proposed system.*

Keywords - *Automatic Generation Control, Fractional Order Controller, Wind system, BESS, Optimization*

I. INTRODUCTION

By making generation, transmission, and distribution independent of each other, the restructured power system is a far more efficient and dependable model than the present power grid. Aside from that, the reformed power system offers a variety of additional services to its consumers. Frequency control is one of its services, which involves matching power output to load needs and therefore decreasing frequency variations. Frequency is important for the functioning of the electrical grid since it adds to system stability. The impact of renewable energy sources on the restructured Automatic Generation Control scheme is investigated in this study. In a two-area power system, extra Wind energy and Battery Energy Storage System (BESS) are combined with traditional non-reheat thermal units to swiftly minimize frequency deviations and evaluate system dynamics.

II. REVIEW OF RELATED STUDIES

The literature discusses parameters involving restructured power system modeling, control & optimization strategies, and RES (Renewable Energy Sources) Injection. The performance analysis and sensitivity analysis were made for AGC with PID controller, and FOPID controller has been compared (Asit Mohanty 2017) .In the article (Yogendra Arya 2017) a restructured power system with energy storage units, the design and execution of an optimum controller (OC) for AGC interconnected two-area power systems are studied. The literature emphasizes that the Battery Energy Storage (BES) has a lot of promise for enhancing the execution of automated generation control (AGC) in power systems by allowing for rapid active power adjustment with a PI controller improved by GA and BFA algorithms are studied by authors in (Pingping Xie 2017). (Yan 2021) discusses a self-adapting control strategy to improve the AGC performance with BES. In the article (Sharma 2018) , for adjusting the gains of PIDF and proportional-integral (PI) controllers, a recently developed novel metaheuristic method called MFO has been recommended. The robustness analysis for the optimal proposed controller also has been performed. In a restructured power system, the performance of a FOPID

controller used for frequency regulation was investigated. The Moth Flame Optimization method (MFO) is used to optimize the controller gains, using the Integral Time Absolute Error (ITAE) as the objective function in (Jennathu Beevi S. 2019) . Energy storage systems are utilized in this study (Arya 2019), to improve the dynamic performance of the WTG model with a classical controller. In (Liu, et al. 2017) frequency regulation with wind energy penetration using switching angle controller has been experimented. Frequency Regulation for the multi-area system with AGC with FOPI controller was optimized by ALO, MFO, WOA, SCA and proven that FOPI with MFO exhibit good performance in (Jennathu Beevi.S 2020), The authors in (Prasun Sanki 2021) optimized AGC controller with MFO. The performance of the AGC controller is compared with GA tuned classical controller with WTG injection (Hakimuddin 2020) When injecting the WTG model, and the performance was analyzed. The literature review shows that the inclusion of BESS and Wind systems has an increased effect on the active power adjustment in frequency control. The authors (Xilin Zhao 2018) discuss wind power participation in a multi-area system. And through involving FOPID controllers optimized with a new MFO algorithm, we would expect to improve the frequency control of our proposed Non-Reheat two-area thermal system.

III. OBJECTIVES OF THE STUDY

- To simulation of AGC with an injection of BESS and wind sources using FOPID controller with unilateral and bilateral contract framework in two area control system.
- To use Objective function ISE (Integral Square Error)to obtain gains values using two algorithms to evaluate and compare the effectiveness of the MFO algorithm proposed for the current system.
- To analyze the impact caused by adding the BESS and wind energy system into the two areas Non reheat thermal system through frequency deviation comparison.

IV. PROPOSED SYSTEM

The power system with two-area frequency control linked with tie lines is shown in Figure.1. The objective is to manage each area's frequency while also controlling the tie-line power. A two-area system with two Gencos and two Discos in each area is proposed for the project under study. In Area-1, Genco 1 is non-re-heat thermal, and Genco 2 is Wind Energy System. In Area-2, Genco 3 is non-re-heat thermal, and Genco 4 is Battery Energy Storage System (BESS). The wet steam coming from the turbine is not used for further processes in the power plant; such a system is called a non-re-heat thermal power system. A non-re-heat thermal power system incorporates a Governor and Turbine. The main controller of the hydraulic turbine is the governing system or governor. To manage the turbine's speed or power generation, the governor regulates the water flow through it. The governor can change the speed of the generators and the frequency of the system. Here a contract load is given, which is the power purchased from the Genco to supply the required load to the Disco approved by the ISO. A tie-line helps to transfer power between area 1 and area 2.

Genco and Disco are each separate entities. The Discos get to choose from which pool of Gencos they want to choose power from, which can be within the area called Unilateral Contract and outside the area called Bilateral contract. This type of multiple power contract scenario raises a lot of confusion in assigning power contracts. Hence the DPM matrix is introduced to make contract participation a lot easier. The Discos can even share their requirement between two sets of Gencos if necessary, and that could also be easily brought into proper representation using the DPM matrix.

As DPM is a matrix representation, it involves rows and columns. Where rows are represented by Gencos and Columns by Discos, and the number of rows is equal in the model. The two-area interconnected power system where there is Genco 1, Genco 2, Disco 1 & Disco 2 in Area 1 and Genco 3, Genco 4, Disco 3 & Disco 4 in Area 2 are considered.

DPM matrix can be represented by Equation 1 as,

$$DPM = \begin{bmatrix} cpf_{11} cpf_{12} cpf_{13} cpf_{14} \\ cpf_{21} cpf_{22} cpf_{23} cpf_{24} \\ cpf_{31} cpf_{32} cpf_{33} cpf_{34} \\ cpf_{41} cpf_{42} cpf_{43} cpf_{44} \end{bmatrix} \quad (1)$$

Where cpf_{jd}=Contract Participation factor of jth Genco in supplying the load of dth Disco. The Disco Participation Matrix (DPM) displays a DISCO's participation in a contract with any GENCO.

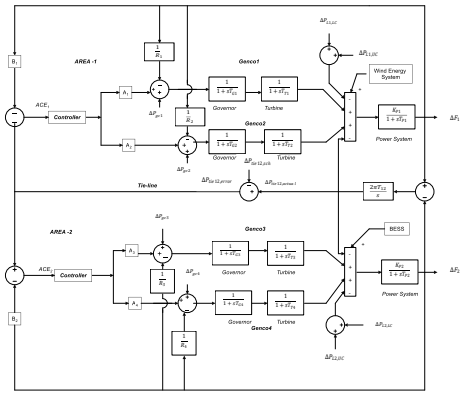

Figure.1: Interconnected two-area system in a deregulated environment

The supplemental control must keep the total interconnected power with nearby areas at planned rates in addition to controlling area frequency. In the additional

feedback loop, this is usually achieved by adjoining a tie line course aberration to the frequency aberration. It's the divergence between scheduled & real power generation in a control region, adjusted for frequency bias.

ACE for two areas is given by Equations. 2 & 3 as,

$$ACE_1 = B_1\Delta f_1 + \Delta P_{tie12} \quad (2)$$
$$ACE_2 = B_2\Delta f_2 + \Delta P_{tie21} \quad (3)$$

B_1&B_2 are frequency bias factors in area 1 and area 2, Δf_1& Δf_2 are the frequency deviations of area 1 and area 2. ΔPtie12 is the real power exchange between area 1 and area 2, respectively. It is represented in the above Equation 4,

$$\Delta P_{tie12}(s) = 2\pi T_{12}/s \quad (4)$$

T_{12} is the time constant for the tie-line connecting areas1&2.

The transfer function of the elements for a two-area power system and the nominal values of the parameters used are given in the appendix.

The tie line error is given in equation 5,

$$\Delta P_{tie12,error} = \Delta P_{tie12,scheduled} - \Delta P_{tie12,actual} \quad (5)$$

The tie-line error reaches zero at a steady state because the actual tie-line power flow equals scheduled power flow. In the conventional situation, an error signal is utilized for creating appropriate area control error signals.

A. FOPID Controller

Fractional-order proportional-integral-derivative (FOPID) controllers have gotten extensive consideration over the course of recent years, both according to scholastic and industrial perspectives. In fact, because they have five parameters to choose from, they provide greater versatility in the controller design than ordinary PID controllers (instead of three). This does, however, imply that the controller's tuning might be much more difficult. PID controllers have been used to eliminate frequency inaccuracy in the majority of the literature. In recent years, there has been a surge in interest in fractional-order controllers, which has sparked a slew of new challenges in the area. Despite the PID controller's excellent dynamic performance, alternative regulators such as Fractional Order PID controllers have been used for frequency management in both traditional vertically integrated utilities and restructured power structures.

Additional parameters in fractional order controllers are generally used to alter and adapt the controller to the demands of the system. As a result, there will be more flexibility to design the controller exactly and precisely to match the system's needs. Recently fractional order controllers have been found to be effective than integer-order controllers. Hence FOPID controller is applied on the proposed system before and after the inclusion of Wind and BES systems. The differential equation of FOPID is given as,

$$G_c(s) = -\left[K_p + \frac{K_i}{S^\lambda} + K_d S^\mu\right] e(t) \quad (6)$$

There are five specifications (K_p, K_i, K_d, λ and μ)which increase pliability to fulfill fixed-configuration requirements such as static errors, phase and gain margins, and resilience. The goal of this project is to develop a practical FOPID controller that meets the design requirements while displaying high efficiency. The basic goal is to find approximations for differential operators that are acceptable for λand μ.

B. Objective Function

ISE is utilized as an objective function (J) for optimizing the gain of a FOPID controller.

$$J = ISE = \int_0^T (\Delta f_1^2 + \Delta f_2^2 + \Delta P_{tie_{12}}^{\ 2})dt \quad (7)$$

If Δf1 is the system frequency variance in area 1 and Δf2 is system frequency variance in area 2. ΔP_{tie} represents an incremental change in tie line & t denotes simulation time interval. Constraints are limits on the controller gains. As a result, the plot might have issues stated as minimize J, subjected as,

$K_{plb} \le K_p \le K_{pub}$ (8a)
$K_{ilb} \le K_i \le K_{iub}$ (8b)
$K_{dlb} \le K_d \le K_{dub}$ (8c)
$\lambda_{lb} \le \lambda \le \lambda_{ub}$ (8d)
$\mu_{lb} \le \mu \le \mu_{ub}$ (8e)

C. Moth Flame Optimization Algorithm (MFO)

Moths glide during the night with the help of the Moon using a transverse orientation mechanism. The primary moth population is created at random, and the assessment norm used to compare best moths with finest flames corresponds to the highest optimal assessment.

Generally, the flame is updated such that moths don't lose their secure solutions &may continue to serve as a "flag". Parameters of the flame matrix, spiral motion & moth matrix change with each iteration.

The d dimension issues are used for optimization in the search domain with n decision variables and values. The populace of N moths acts as a gateway with d dimensional vector assess, where every moth acts like an agent. Moths travel in the d dimensional space, and potential solutions are their positions. Moths navigate in d dimensional area, where their positions are potential solutions. The collection and locations of the moths are described by the n ×d matrix in Equation 9.

$$M = \begin{bmatrix} M_{11} & M_{12} & \dots M_{1d} \\ M_{21} & M_{22} & \dots M_{2d} \\ \vdots & \vdots & \vdots \\ M_{n1} & M_{n2} & \dots M_{nd} \end{bmatrix} \quad (9)$$

The moths' collection and locations are described in the n× d matrix below,

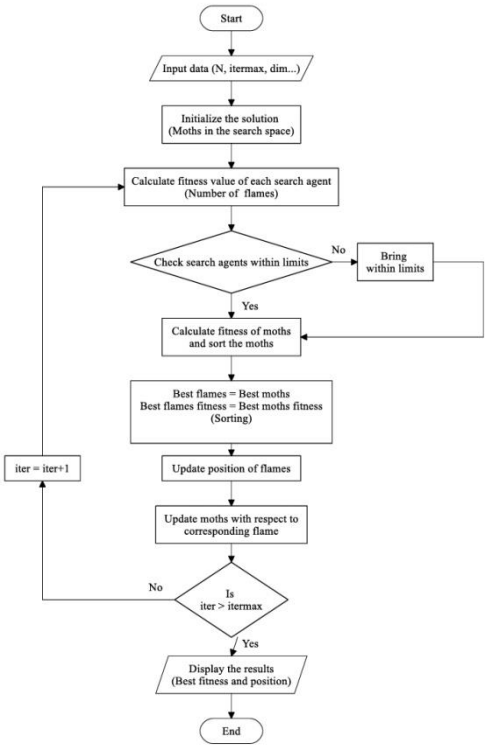

Figure. 2: Moth Flame Optimization Flowchart

$$OM = \begin{bmatrix} OM_1 \\ OM_2 \\ \vdots \\ OM_n \end{bmatrix} \quad (10)$$

The flames are shown in the matrix below

$$F = \begin{bmatrix} F_{11} & F_{12} & \dots F_{1d} \\ F_{21} & F_{22} & \dots F_{2d} \\ \vdots & \vdots & \vdots \\ F_{n1} & F_{n2} & F_{nd} \end{bmatrix} \quad (11)$$

The fitness values of fames are kept in an OF vector.

$$OF = \begin{bmatrix} OF_1 \\ OF_2 \\ \vdots \\ OF_n \end{bmatrix} \quad (12)$$

From a mathematical standpoint, MFO is divided into three parts:

$$MFO = (I, P, T) \quad (13)$$

Where P is the refurbishment term, T is the elimination term, and I is an attribute that alters the populace of moths and their fitness values. On the choice of variables such as upper bound and lower bound.

$$ub = [ub_1, ub_2, \dots, ub_d] \quad (14)$$

$$lb = [lb_1, lb_2, \dots, lb_d] \quad (15)$$

D. Battery Energy Storage System (BESS)

BESS is a potential innovation because of its inherent dispersed nature, capability to inoculate biface power movement, peak power scaling & capacity to furnish a variety of grid functions. BESS is used to provide a variety of services in today's environment, including peak shaving, energy management of microgrids, and debatable assets, and frequency &voltage regulation. The considerable cost of these gadgets has thus far hindered their implementation. While this cost is decreasing as a result of technology advancements, one practical proposal is to cope with it is to build control techniques that can deliver many services at the same time. From a technological and economic standpoint, this considers BESS use. The simultaneous provision of various services via BESSs is of particular relevance from two perspectives. Varying applications demand different amounts of energy and power. Some are "energy-demanding," requiring a large amount of energy but having a modest immediate power (for example, peak shaving). Others are "energy-demanding," requiring higher amounts of power but not a large quantity of energy (for example, primary frequency regulation). These numerous services might be combined to match the energy &power rating of the batteries as closely as possible. Batteries offer a single amenity for an extended period of time, however, because of the unpredictability of the debatable assets with connected loads.

As a result, deploying such services seldom necessitates the full utilization of the BESS function. Then the leftover BESS energy function after the primary service is deployed, it can be given to a subordinate amenity which will be deployed parallel. Overall, combining several services may allow, in the best-case situation, to leverage the batteries in combination with stochastic processing. A power transformer, battery bank, and an AC-DC converter are linked to the power grid, where the control method is used to make up a BESS. A diagram of the BES system may be obtained. The BES can deliver fast changes in active power in both directions with a proper control system, and therefore may be utilized to provide a supplemental AGC function. The transfer function of the control system is the most important consideration in AGC modeling and analysis. As shown in Figure 3, we developed a BES control diagram model for AGC analysis, where K_{pb} is the gain of balance power, T_{ch} is the time constant of balancing charge, K_b is the feedback gain of frequency fluctuation, and T_{conv} is the time constant of the power converter. The frequency variation in region i is Δf_i, and the BES power output is P_b. The balancing charging loop in this model may simulate the frequency response behavior of BES &keep leftover energy in the starting condition (represented by K_{pb} and T_{ch}). $\frac{K_{pb}}{T_{Charge}s+1}$ depicts a battery energy storage system's auto-balancing charging loop. This loop might regulate the energy storage's remaining energy around the original condition, which is usually said to be 50%. The feedback gain of

frequency fluctuation in the electrical grid is represented by the symbol K_b. With BESS, it reflects the impact of a first-order delay in the dc to the ac power converter.

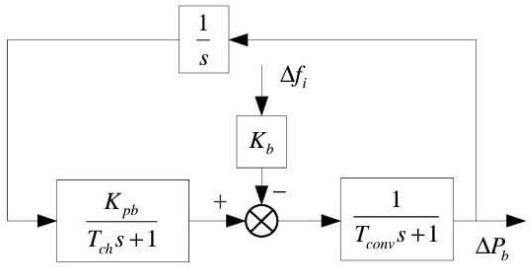

Figure.3: Control Diagram of BESS system

E. Wind Energy System

Renewable energy has experienced a lot of recognition in recent decades due to the rising expense of fossil fuels and their negative impact on the environment. Wind energy is the fastest-growing renewable energy source among them. The Indian wind energy sector is led by the country's own wind energy industry, which has experienced consistent expansion. The government is enticing private sector participation in wind power projects around the country by providing tax & monetary incitement like accelerated depreciation and custom duty exemptions on specified elements of wind energy turbines. Individual WTG responses must be modeled in order to understand the collective dynamics involved in wind farms. The mathematical model of a wind farm with hundreds of WTGs can involve a considerable number of differential equations, which will require significant processing power and time to solve. As a result, when modeling the dynamics of such huge systems, aggregate models are commonly used. Instead of several WTGs, the entire wind farm can be reduced to a single large WTG or a limited number of large WTGs utilizing aggregation models. Due to the spatial distribution of WTGs in wind farms, each WTG will experience a different wind speed at any given time, resulting in no two WTGs having the same output. In the present work, at constant wind speed, an empirical transfer function between frequency error and WTG output is established. At a wind speed of 12 m/s, the response of the nonlinear reloaded WTG model (K.V. Vidyanandan n.d.) is considered in the present work, and its linearized transfer function for a slight step increase in frequency (0.01 pu) is given by Equation 16. The response of the linearized model is quite close to that of the non-linear model for small frequency errors, confirming the accuracy of the transfer function representation.

$$G(s) = \frac{-49.2611s - 2.4897}{49.2611\,s + 1} \qquad (16)$$

V. IMPLEMENTATION AND SIMULATION RESULTS

The efficacy of the suggested PID and FOPID controllers for a 2-area non-reheat thermal power system is demonstrated in this section. The system parameters utilized for simulation are listed in the "Appendix."The tables and graphs below show the optimal outcomes for the three scenarios that were optimized using optimization techniques. All of the scenarios' quantitative comparisons are listed here. The performance of all the Algorithm-optimized situations is presented.

A. Scenario 1

The two areas non reheat thermal system with Windpower and Battery Energy Storage System(BESS) has been considered. A PID controller is optimized using Genetic Algorithm(GA) and Moth Flame Optimization(MFO) with Integral Square Error(ISE) as an objective function to minimize the error value. The lower bound and upper bound for the controller gains K_p, K_i, K_d is given as 0.01 and 5 for the PID controller. Once the fitness function, the number of variables, lower bound, and upper bound are given in "gatool", the algorithm is then simulated to analyze the performance characteristics.

a) Unilateral Market Structure

The PID controller was optimized by two optimization algorithms, namely genetic algorithm (GA) and Moth Flame optimization(MFO) algorithm, while injecting WIND & BESS system in the two area system for the unilateral market model. The controller gain values Kp, Ki, Kd values are compared and shown in Table 1

TABLE.1: GAINS OF PID CONTROLLER USING GA AND MFO ALGORITHM

PID GAINS	OPTIMIZED USING GA	OPTIMIZED USING MFO
Kp1	4.8737	2
Ki1	0.0344	0.1000
Kd1	1.6881	1.7697
Kp2	2.5583	2
Ki2	0.1584	0.1000
Kd2	1.3359	1.3825
ISE	0.00010544	0.00011229

The output responses obtained by simulating with the optimized gains are given in Figure.4 - Figure.6. Figure. 4 compares the changes in area-1 frequency obtained by a PID controller optimized by GA and MFO algorithms. Figure.4 shows the steady-state frequency change in area-1 after the inclusion of wind and BESS along with the PID controller. Figure.5 depicts the steady-state frequency change in area-2 after the inclusion of wind and BESS along with the PID controller. Figure.6 displays the steady-state tie-line power deviation between area-1 and area-2 after the inclusion of wind and BESS along with the PID controller. PID controller

has been optimized by GA & MFO algorithm. In area 1, the GA gives ST as 4.2s, but MFO gives the ST as 3.5s. Similarly, In area 2, the GA gives ST as 6.1s, but MFO gives the ST as 4.5s. From all these comparisons from the table, it is clearly observed that the MFO algorithm with PID controller exhibits competitive performance.

TABLE.2: COMPARISON OF PERFORMANCE CHARACTERISTICS FOR PID CONTROLLER OPTIMIZED USING GA AND MFO ALGORITHM - UNILATERAL MARKET

Control Area	Performance Measures	Optimized Using GA	Optimized Using MFO
Area 1	OS	0.0212	0.0112
	US	-0.0504	-0.0506
	ST	4.2	3.5
Area 2	OS	0.00276	-0.0005
	US	-0.0121	-0.0124
	ST	6.1	4.5

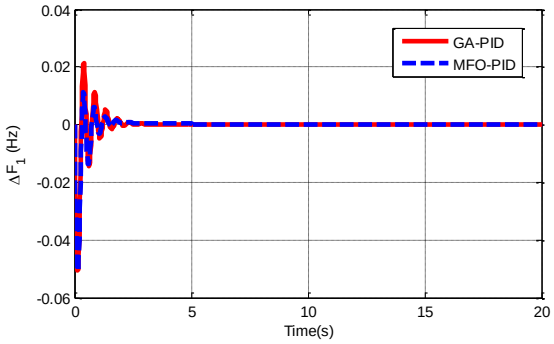

Figure.4: Comparison of GA and MFO for frequency change in area 1 (Δf_1) with Wind and BESS, employing PID controller - Unilateral Market

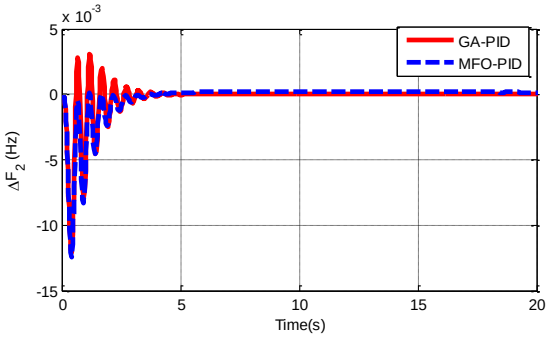

Figure.5: Comparison of GA and MFO for frequency change in area 2 (Δf_2) with Wind and BESS, employing PID controller - Unilateral Market

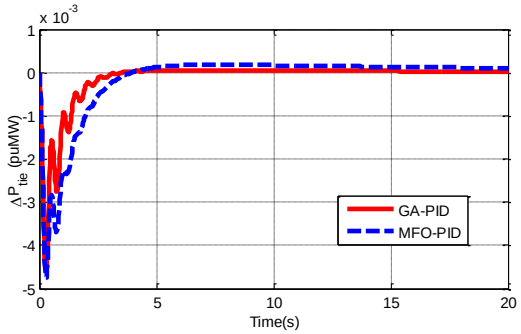

Figure.6: Comparison of GA and MFO for Tie Line power deviation between area 1 & area 2 (ΔP_{tie}) with Wind and BESS, employing PID controller - Unilateral Market

b) Bilateral Market Structure

The PID controller was optimized by two optimization algorithms, namely genetic algorithm (GA) and Moth Flame optimization(MFO) algorithm while injecting WIND & BESS system in the two area system for the bilateral model. The controller gain values Kp, Ki, Kd values are compared and shown in Table.3.The Comparison of GA and MFO for frequency change in the area shows a fig 7 and 8. The Comparison of GA and MFO for Tie Line power deviation between area 1 & area 2 shows fig 9.

TABLE.3: GAINS OF PID CONTROLLER USING GA AND MFO ALGORITHM

PID Gains	GA	MFO
Kp1	4.9589	2
Ki1	0.1239	0.1000
Kd1	1.7088	1.7820
Kp2	2.5603	2
Ki2	0.1116	0.1000
Kd2	1.3474	1.3740
ISE	0.00039307	0.00040194

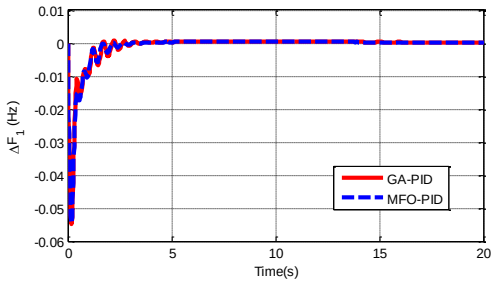

Figure 7: Comparison of GA and MFO for frequency change in area 1 (Δf_1) with Wind and BESS, employing PID controller - Bilateral Market

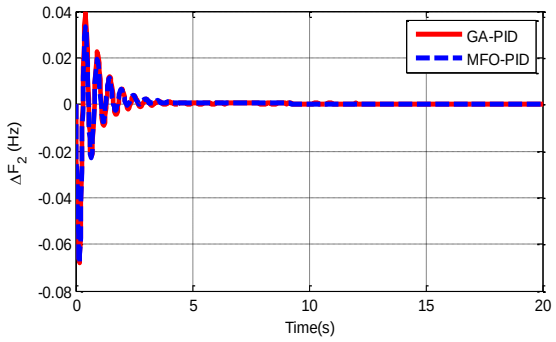

Figure. 8: Comparison of GA and MFO for frequency change in area 2 (Δf_2) with Wind and BESS, employing PID controller - Bilateral Market

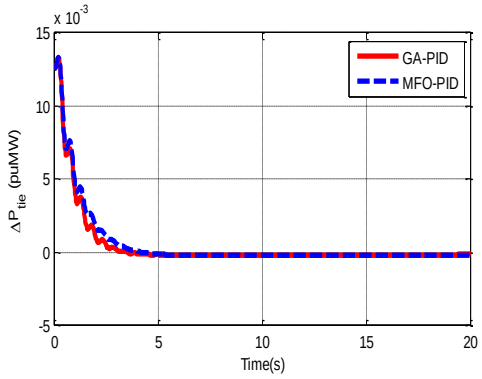

Figure.9: Comparison of GA and MFO for Tie Line power deviation between area 1 & area 2 (ΔP_{tie}) with Wind and BESS, employing PID controller - Bilateral Market

TABLE.4: COMPARISON OF PERFORMANCE CHARACTERISTICS FOR PID CONTROLLER OPTIMIZED USING GA AND MFO ALGORITHM - BILATERAL MARKET

Control Area	Performance Measures	GA	MFO
Area 1	OS	-0.0108	-0.0151
	US	-0.0549	-0.0546
	ST	6	4.7
Area 2	OS	0.0394	0.0335
	US	-0.0678	-0.0679
	ST	6.6	5.6

B. Scenario 2

The two areas non reheat thermal system with Windpower and Battery Energy Storage System(BESS) and without Wind and Battery Energy Storage System (BESS) system has been considered. The three-term controller and FOPID controller are optimized using Moth Flame Optimization(MFO) with Integral Square Error(ISE) as an objective function to minimize the error value of the controller. The lower bound and upper bound for the controller gains k_p, k_i, $k_d$is given as 0.01 and 5 for the PID controller The lower bound and upper bound for the controller gains k_p, k_i, $k_d$is given as 0.01 and 2 and for the additional gains λ, μ values are between 0.5 and 1.5 for the FOPID controller. The search agents in the optimization algorithm are given as 100. An iteration of 100 is given for the system. Here the classical controller is compared with fractional order controller, which is optimized by MFO to prove yhe effectiveness of the controller.

a) Unilateral market structure with Wind and BESS injection

The MFO algorithm was used to optimize the FOPID controller and PID controller while incorporating the WIND & BESS system for the unilateral model. The controller gain values Kp, Ki, Kd, Kλ, Kμ values are compared and shown in Table.5.

TABLE.5: GAINS OF PID CONTROLLER AND FOPID CONTROLLER USING MFO ALGORITHM - UNILATERAL

GAINS	FOPID OPTIMZED USING MFO	PID OPTIMIZED USING MFO
Kp1	2	2
Ki1	2	0.1000
Kd1	2	1.7697
λ1	0.5000	-
μ1	1.0791	-
Kp2	2	2
Ki2	-0.0100	0.1000
Kd2	2	1.3825
λ2	1.5000	-
μ2	1.3680	-
ISE	0.000091495	0.00011229

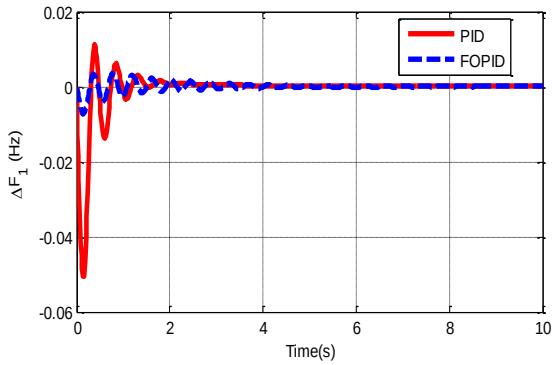

Figure.10: Frequency change in area 1 (Δf_1) for PID and FOPID controller optimized by MFO.

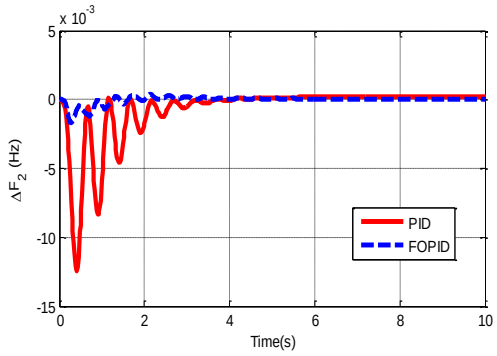

Figure.11: Frequency change in area 2 (Δf_2) for PID and FOPID controller optimized by MFO

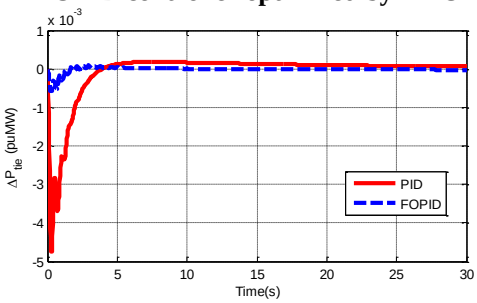

Figure.12: Tie line power deviation (ΔP_{tie}) for PID and FOPID controller optimized by MFO.

Interpretation of Figure.10,11,12.

In this case, FOPID controller and PID controller were optimized by the MFO algorithm while incorporating the WIND & BESS system for the unilateral model. In area 1, PID-MFO gives the ST of 6s and FOPID-MFO gives the ST of 5s, which is better than the PID controller. Similarly in area 2, PID-MFO gives the ST of 13s and FOPID-MFO gives the ST of 9s, which is better than the PID controller. The performance characteristics are shown in Table 6.

TABLE.6.COMPARISON OF PERFORMANCE CHARACTERISTICS FOR PID AND FOPID CONTROLLERS OPTIMIZED USING MFO ALGORITHM – UNILATERAL

CONTROL AREA	PERFORMANCE MEASURES	FOPID OPTIMIZED USING MFO	PID OPTIMIZED USING MFO
AREA 1	OS	0.00675	0.0112
	US	-0.04975	-0.0506
	ST	5	6
AREA 2	OS	-0.00524	-0.0005
	US	-0.0108	-0.0124
	ST	9	13

b) Bilateral market structure with Wind and BESS injection

The MFO algorithm was used to optimize the FOPID controller and PID controller while incorporating WIND and BESS systems for the unilateral model. The controller gain values Kp, Ki, Kd, λ, μ values are compared and shown in Table 7.

TABLE.7: GAINS OF PID CONTROLLER AND FOPID CONTROLLER USING MFO ALGORITHM.

GAINS	FOPID OPTIMZED USING MFO	PID OPTIMIZED USING MFO
Kp1	2	2
Ki1	1.3895	0.1000
Kd1	2.0000	1.7820
λ1	0.5000	-
μ1	1.0716	-
Kp2	2	2
Ki2	2	0.1000
Kd2	1.6173	1.3740
λ2	0.5000	-
μ2	1.0800	-
ISE	0.000033049	0.00040194

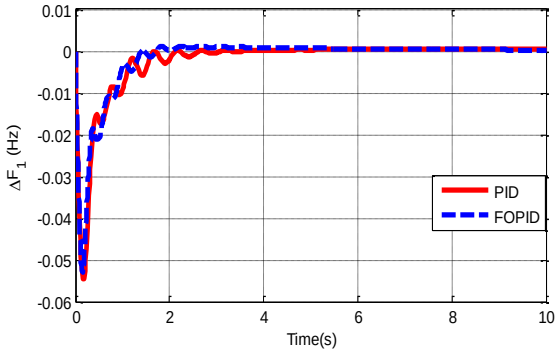

Figure.13: Frequency change in area 1 (Δf_1) for PID and FOPID controller optimized by MFO

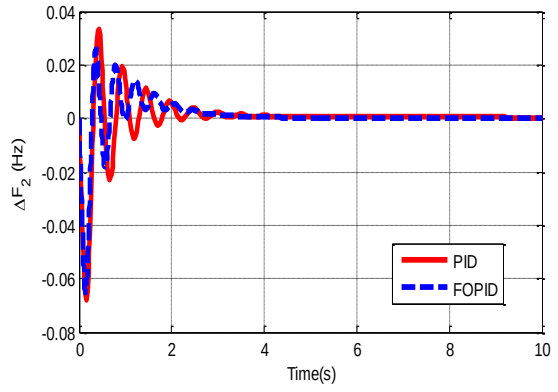

Figure.14: Frequency change in area 2 Δf_2) for PID and FOPID controller optimized by MFO

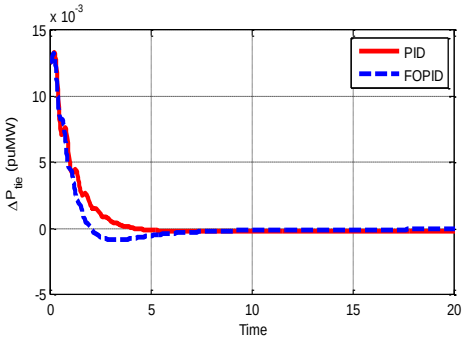

Figure.15: Tie-line power deviation(ΔP_{tie}) for PID and FOPID controller optimized by MFO

Interpretation of Figure.13,14,15.

In this case, FOPID controller and PID controller were optimized by the MFO algorithm while incorporating the WIND & BESS unilateral model. In area 1, PID-MFO gives the ST of 10s, and FOPID-MFO gives the ST of 7.5s, which is better than the PID controller. Similarly, in area 2, PID-MFO gives the ST of 7s and FOPID-MFO gives the ST of 5s, which is better than the PID controller. The performance characteristics are shown in Table.8.

TABLE.8.COMPARISON OF PERFORMANCE CHARACTERISTICS FOR PID AND FOPID CONTROLLERS OPTIMIZED USING MFO ALGORITHM

CONTROL AREA	PERFORMANCE MEASURES	FOPID	PID
AREA 1	OS	-0.0185	-0.0151
	US	-0.0528	-0.0546
	ST	7.5	10
AREA 2	OS	0.026	0.0335
	US	-0.0655	-0.0679
	ST	5	7

VI. CONCLUSION

A two-area system with non-reheat thermal units and a wind energy system in area-1 and a non-reheat thermal system with a battery energy storage system in the second area has been considered. Initially, the PID controller has been applied, and the gains of the system are optimized using two optimization algorithms, namely GA & MFO. The optimization algorithms are used since the conventional methods are complex & aren't accurate. From the comparison of the output curves, it has been observed that the PID controller optimized by MFO gives the best results. Then, the FOPID controller is applied to the proposed system after the inclusion of Wind and BES systems. The performance of PID & FOPID controllers using the MFO algorithm has been compared. From the results, it has been found that the system with wind & BESS using FOPID controller gives better results. This validates the feasibility of including the DFIG and energy storage system in a multi-area restructured power system.

REFERENCES

[1] Y. Arya. Effect of energy storage systems on automatic generation control of interconnected traditional and restructured energy systems. International Journal of Energy Research, 43(12) (2019) 6475-6493.

[2] A. Mohanty, D. Mishra, K. Mohan, P.K. Ray, and S.P. Mohanty, Optimised fractional order PID controller in automatic generation control. In Computer, Communication and Electrical Technology (2017) 215-219.

[3] N. Hakimuddin, I. Nasiruddin, T.S. Bhatti, and Y., Arya. Optimal Automatic Generation Control with Hydro, Thermal, Gas, and Wind Power Plants in 2-Area Interconnected Power System. Electric Power Components and Systems, 48(6-7) (2020) 558-571.

[4] S.J. Beevi, and R. Jayashree, Optimal Fractional Order PID Controller for Centralized and Decentralized Frequency Control in Restructured Power System.

[5] J.B. Sahul Hameed, and J. Ramasubramanian. Optimal Fractional Order PI Controller for Frequency Ancillary Services in Restructured Power System. Energy Systems, (2020) 1-31.

[6] K.V. Vidyanandan, and N. Senroy, Simplified dynamic models of variable speed wind turbines for frequency regulation studies. In 2013 IEEE Innovative Smart Grid Technologies-Asia (ISGT Asia) (2013)1-6. IEEE.

[7] Y. Liu, L. Jiang, Q.H. Wu, and X. Zhou, "Frequency control of DFIG-based wind power penetrated power systems using switching angle controller and AGC". IEEE Transactions on Power Systems, 32(2)(2016)1553-1567.

[8] Optimal Fractional OrderPI controller for Frequency Ancillary Services in Restructured Power System.Energy Systems, Springer Nature, (2020).

[9] P. Xie, J. Zhu, and P. Xuan, Optimal controller design for AGC with battery energy storage using bacteria foraging algorithm. In 2017 IEEE Power & Energy Society General Meeting (2017) 1-1.

[10] P. Sanki, M. Basu, P.S. Pal, and D. Das. Application of a novel PIPDF controller in an improved plug-in electric vehicle integrated power system for AGC operation. International Journal of Ambient Energy, (2021) 1-15.

[11] M. Sharma, R.K. Bansal, S. Prakash, and S. Dhundhara, December. Frequency regulation in PV integrated power system using MFO tuned PIDF controller. In 2018 IEEE 8th Power India International Conference (PIICON) (2018) 1-6.

[12] X. Zhao, Z. Lin, B. Fu, L. He, and N. Fang. Research on automatic generation control with wind power participation based on predictive optimal 2-degree-of-freedom PID strategy for a multi-area interconnected power system. Energies, 11(12) (2018) 3325.

[13] L. Yan, J. Mei, P. Zhu, B. Zhang, and X. Chen, A self-adapting Control Strategy to Improve Performance of AGC with Battery Energy Storage System (BESS). In 2021 IEEE 4th International Electrical and Energy Conference (CIEEC) (2021) pp. 1-6.

[14] Y. Arya, N. Kumar, and S.K. Gupta. Optimal automatic generation control of two-area power systems with energy storage units under deregulated environment. Journal of Renewable and Sustainable Energy, 9(6) (2017)064105.